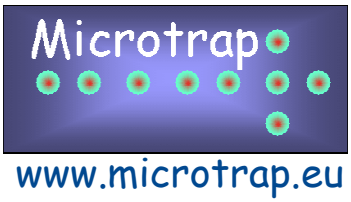

MICROTRAP

Development of a pan-European Microtrap Technology capability for Trapped Ion Quantum Information Science

Final Summary Report

Project acronym:	MICROTRAP
Project no:	IST-517675
Instrument:	STREP
Thematic Priority:	IST FET
Start date:	1st April 2006
Duration:	3.5 years
Reporting Period:	1 April 2006 – 30 September 2009
Co-ordinator:	Professor Patrick Gill NPL Management Ltd Teddington TW11 0LW, UK

Partner number and acronyms:

1.NPL	National Physical Laboratory, Teddington, UK
2.UIBK	University of Innsbruck, Austria
3.UAAR	University of Aarhus, Denmark
4.UOXF	Oxford University, UK
5.USIEG	University of Siegen, Germany
6.UULM	University of Ulm, Germany

Contents

Introduction

MICROTRAP is a Strep project developing an EU technology capability in trapped ion micro-structures for application to quantum information science. The major experimental advances in quantum information science over the last decade have all been demonstrated in mesoscopic trapped ion systems, and include qubit operation, deterministic entanglement, basic quantum algorithm demonstration, quantum gate operation and quantum state teleportation. Already, trapped ion technology has been shown capable to meet DiVincenzo criteria for viable quantum computing. These address qubit initialisation, qubit read-out, universal quantum gates, scalability and long coherence times. The last two are critical for achieving an architecture allowing many qubit interactions and thereby capable of competing with CMOS-based computing power. This project targets scalability through miniaturisation of trapped ion architectures, allowing quantum logic manipulation of ion arrays whilst minimising decoherence through environmental perturbation.

The consortium of MICROTRAP partners comprise 6 major trapped ion groups from UK, Austria, Denmark and Germany, and include the leading European experimental trapped ion QIP researchers. This consortium of partners is focused on European micro-machining and micro-fabrication capability to design, develop and test micro-trap architectures.

The MICROTRAP project goal targeted the supply and test of microtrap devices with optimised microtrap materials, trap design and fabrication processes, organised within standard chip mounting architectures. Objectives for the latter part of the project were to test fabricated microtraps for suitability as QIP devices through measurement of ion cooling and heating rates and decoherence, and demonstration of ion shuttling capability, entanglement and gate operations and the potential for scalability.

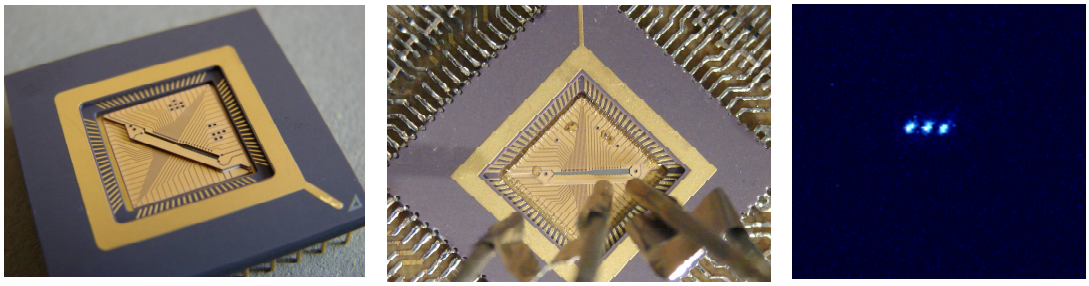

Fig.1*: Prototype gold-coated 3-layer ceramic wafer microtrap, and a 3-ion cold crystal observed with the prototype trap*

The outputs of the project represent a major step forward in integrating QIP into micro-electronics technology, bridging the gap between large, complex laboratory demonstrations and viable microtrap chips. Three microtrap design architectures were pursued during the course of the project. Two designs of three-dimensional traps were investigated; the first was based on gold-coated ceramic wafers, the second on gold-coated silica-on-silicon wafers. The ceramic wafer microtrap has been used to demonstrate several QIP techniques such as sideband cooling, ion transport and Ramsey spectroscopy. In the latter half of the project, gold-on-quartz two-dimensional (surface) traps were also designed, fabricated and operated.

We have also achieved a range of techniques for microtrap mounting on industry-standard chip carriers, allowing easy-access chip connectivity into the ultra-high-vacuum environment needed for the microtrap, and interfacing directly with standard micro-electronics design. This is a “lab-on-a-chip” approach, but with control and manipulation of the quantum state.

Microtraps developed within this project have undergone the initial stages in evaluating suitability for quantum information applications. The all-important parameters of heating and associated decoherence rates have been measured for some of the fabricated microtraps. Elementary operations required for entanglement and gates, such as coherent spectroscopy and precisely controlled ion transport, have also been demonstrated. In achieving this, the project has made significant progress in addressing the scalability challenge that underpins viable trapped ion quantum information processing.

Microtrap design and fabrication

Gold-coated 3-layer ceramic wafer design

The first fabrication concept is based on an Al_20_3 ceramic wafer approach, and was co-ordinated by the University of Ulm. This involves femtosecond fast pulse laser machining of a typical 125 µm-thick wafer to provide sets of upper, lower and intermediate spacer layers which make up the trap. With the basic trap design shape cut into the wafer, the upper and lower layers are gold-coated and electro-plated to provide the trap upper and lower electrode architecture, and then further laser machining is carried out to cut the various tracks within the coating. The two coated layers and spacer layer are aligned and glued to provide the 3-D microtrap chip which is then mounted on a standard chip carrier. During year 1 of the project, it became clear that while the laser cutting of the wafer is relatively straightforward, the evaporative gold coating and subsequent electro-plating presented more of a challenge, and activity to optimise these steps delayed the first phase of microtrap chip production. Nevertheless, Ulm demonstrated successful trapping of a string of single ions within a prototype microtrap chip based on this approach by the end of the first year, confirming the viability of the technology.

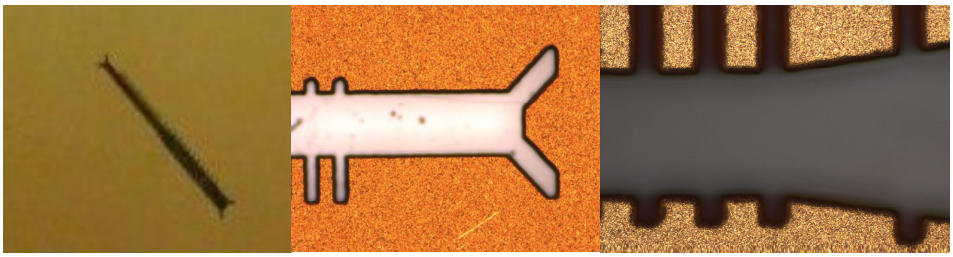

Fig. 2*: shows optical images of the machined and gold-coated linear trap, a close up of the end of the trap, and the taper region after gold plating.*

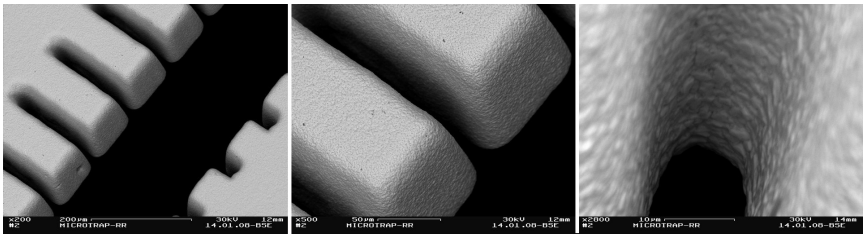

Fig. 3: *electron microscope image of the gold plated chip showing ~ 1 µm roughness due to the ceramic wafer*

During the first two years of the project, significant delays had been experienced in realising the fabrication of the microtrap design concepts. These centred around the efficiency and

yield of certain fabrication steps, and also some scheduling delays from the fabrication companies commissioned to supply to our designs. However, the successful operation of the ceramic wafer prototype trap at the end of year1 represented a major milestone, and this underpinned the optimisation of batch processing steps associated with the underlying 400 nm thick evaporative gold coating layer and subsequent 5 µm-thick electroplating layers. The batch processing was successfully completed at the end of year 2, with the trap component layers corresponding to three different designs (linear trap, linear taper trap and cross trap) distributed to the consortium early in period 3 for layer alignment and bonding, mounting on chip carriers and wire-bonding by the individual partners. During the final period, traps have been assembled by Ulm and Siegen (linear taper design), and Oxford and Innsbruck (cross trap design), with subsequent microtrap operation achieved so far by Ulm and Innsbruck.

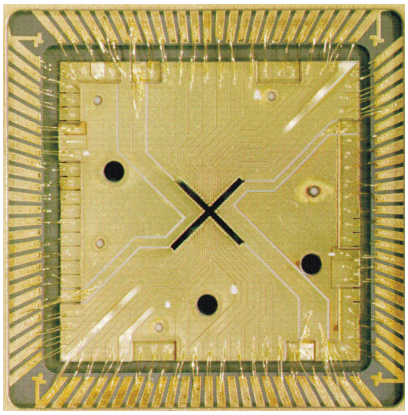

Fig. 4: *Assembled Au-on-Al_2O_3 trap chip containing an X-junction*

In addition to the standard ceramic wafer designs under construction, there has also been additional design activity carried out by the universities of Aarhus and Siegen in order to provide microtrap chip variants. These make use of the standard upper and lower electrode layers, but introduce slightly different spacer layer arrangements. In Aarhus's case, the aim was to develop microtrap designs with a micro-oven for loading ions into the trap embedded into the spacer wall, and activated by means of laser ablation by means of nanosecond laser pulses delivered to the trapping region by optical fibres also embedded in the spacer layer. Siegen concentrated on a microtrap design with an integrated magnetic field gradient for qubit discrimination. This required a thick gold-coated intermediate spacer layer to provide the magnetic field coils, but insulated from the electrode layers. As in the Aarhus case, special spacer layers were machined for these purposes. Laser machining, coating and plating of spacer layers was achieved in parallel with the main batch processing. In addition to the ceramic layer traps machined by Micreon GmbH, Aarhus developed their own in-house capability for fabricating gold-on-ceramic trap chips.

The Siegen variant targets an approach for ion trap based QIP where hyperfine qubits in the electronic ground state are manipulated by microwaves, thus eliminating qubit lifetime issues, as well as spontaneous scattering by Raman transitions. This approach requires state selective forces which can be implemented by a large magnetic field gradient at the ion positions and the ceramic wafer middle spacer of the three layer microtrap design was modified and optimized to achieve maximum gradient per ohmic heating. The current around the edge of the gold-plated middle layer can be understood as a segment of a Maxwell or anti-Helmholtz pair and produces a magnetic quadrupole field.

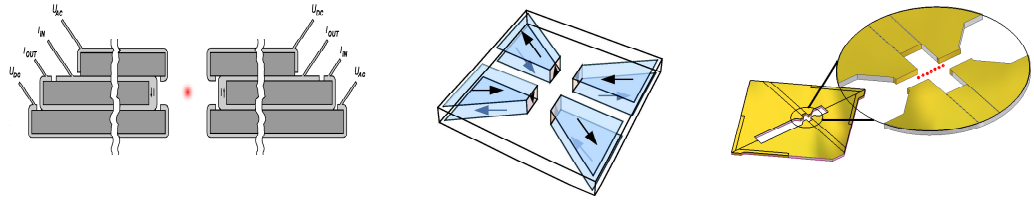

Fig. 5*: Left: Three layer trap structure with current-carrying middle layer for magnetic fields Centre: schematic of current flow through coil structure; Right: actual design of middle layer*

The generated ohmic heat can be carried away efficiently by the good thermal contact to the substrate and aIlows for high current densities of more than $1*10^{11}$ A/m^2. The gold plated spacer layer surface requires insulation from top and bottom layer which was implemented by Kapton foils. A simulated field gradient is shown below.

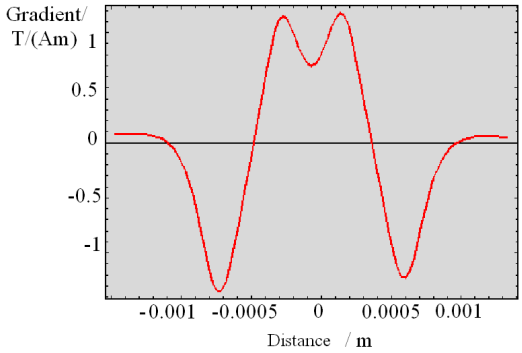

Fig. 6: *Simulated gradients for Siegen middle layer with Ulm ceramic trap design*

The alternative approach at Aarhus incorporates prealigned optical fibers within the microtrap structure itself for delivering the various laser beams required needed for photo-ionisation, cooling and probing the ions. This has benefit for beam quality and stability, and reduced need for free-space optical access to the trapping region. Taking into account the delays with the Micreon trap delivery, Aarhus designed and fabricated a multi-segment microtrap with 4 integrated lensed optical fibres. Two are capable transmitting the repumping light at 866 nm and quadrupole cooling light at 729 nm light for trapping Ca^+ ions, with the other two for delivery of the UV 272 nm photo-ionization light and the 397 nm primary cooling light.

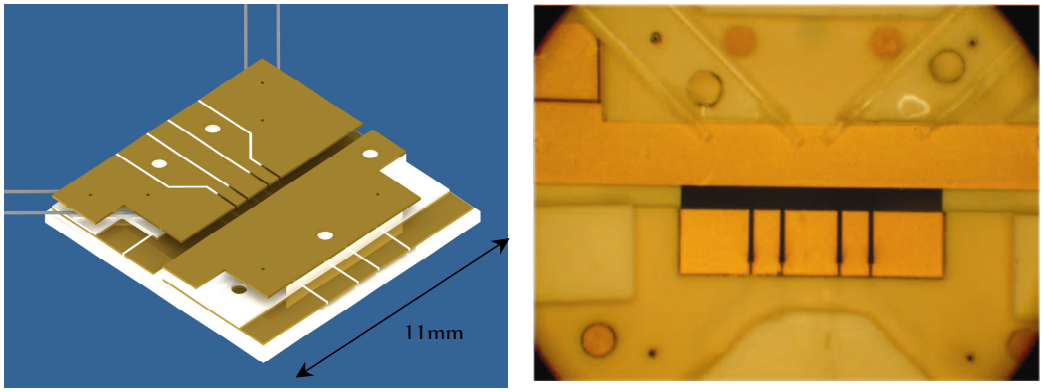

Fig. 7: *Design drawing of the Aarhus laser-machined alumina trap (left) and the assembled lower layer of the trap electrodes showing 4pre-aligned lensed optical fibers.*

One important consideration of the integration of optical fibres is the need to keep them sufficiently far from the trapping region that they do not perturb the trapping field and are not susceptible to charging effects. In the Aarhus trap design they are ~ 1.5mm from the trap axis, and so a lensed fibre with large working distance is required. At short wavelengths, lensed fibres are not available commercially. Two different techniques for manufacturing such fibres have been developed within the project. Aarhus splice a short length of coreless silica fibre onto the single mode fibre end, and which is then melted to form a hemispherical lens surface for focussing. An alternative technique was developed at NPL by using a focused ion beam to mill the silica surface of the fibre end to give a binary Fresnel lens

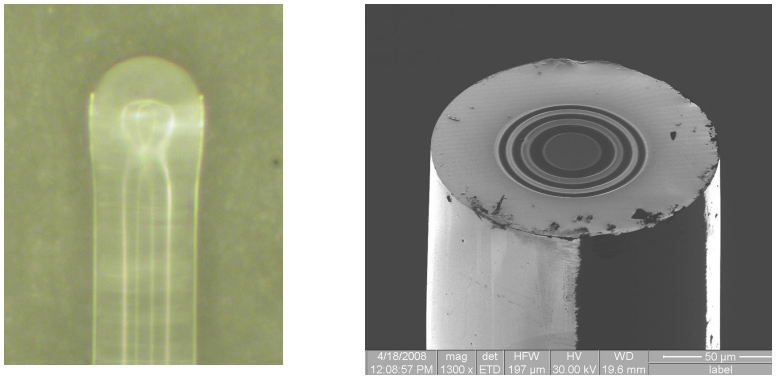

Fig 8: *left, Photograph of a lensed fibre created using Aarhus technique; right, binary Fresnel lens milled into surface of fibre*

Gold-coated silica-on-silicon monolithic wafer trap chip design

The second fabrication methodology is a monolithic concept, allowing significant parallel processing of the chip trap, and offering a viable route to scaleable chip design. It is based on silica ($Si0_2$)-on-silicon wafer technology and has been investigated by NPL. Silicon wafers of typical thicknesses ~350 µm, are oxidised to provide 15 µm-thick silica layers on both sides of the wafer. Subsequent lithographic processing steps include etching through the trap aperture, and gold-coating the etched silica layers to form a multiple-segment electrode architecture. This lithographic fabrication approach offers multiple 3-D trap chips to be produced from a single wafer [1]. This approach is higher risk than the ceramic wafer method, but offers a novel, scalable arrangement in the longer term.

During the first year, NPL undertook a prototyping activity with a fabricator in order to determine the optimal processing parameters. This pre-production test and analysis showed that certain critical processing steps needed optimisation before acceptable trap chip fabrication was viable. These stem mainly from the need to adapt standard 2-D surface etching lithographic fabrication methods to the 3-D etch-through and under-etch requirements needed for the microtrap. As a result, there were significant delays to fabrication, with result that NPL recruited a micro-fabrication specialist to optimise the process steps. Wafer processing that built on established process steps were outsourced to a fabricator with appropriate experience, whilst the application of process steps to the novel etch-through and undercut approach was developed in-house at NPL at individual chip level.

The ideal design of the monolithic ion trap is now achieved with modified versions of standard fabrication techniques. The first two relatively straightforward processing steps (*i.e.* metallisation and SiO_2 etch) were conducted at wafer level. NPL then developed the processing steps for through-etching of the Si, followed by undercut etch-back of the Si by ~

[1] M Brownnutt et al., New J. Phys. **8** 232 (2006)

220 µm below the electrode segments. This was followed by shadow evaporation into the undercut and electroplating of outside and underside coated surfaces. This development work has been successful in demonstrating a complete fabrication process required to achieve the ideal undercut structure for a 3D monolithic trap chip (figure 2). The combination of all required processing steps into a complete sequence represented a major fabrication challenge; however trap chips resulting from this work are now under test. This structure is one of only two monolithic 3D trap designs made using micro-fabrication techniques.

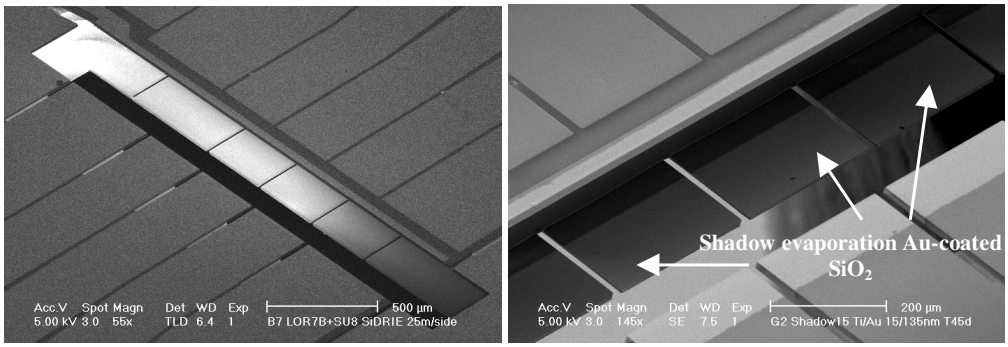

Fig. 9. *SEM images of electrode structure in the 3D monolithic ideal trap. Left, the SiO_2 inside the aperture is uncoated, resulting in charge build up to give a bright SEM image; Right, with shadow evaporation completed on the underside of the silica.*

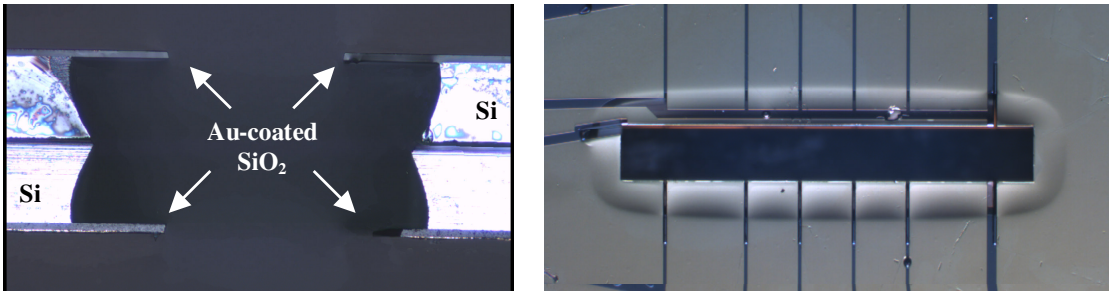

Fig 10: *Left: Cross-section of an individual trap chip aperture after the isotropic Si etch. The trap chip was diced through the aperture to reveal the profile of the gold-coated SiO_2 (electrodes) and the silicon substrate. The recess depth is around 220 µm. Right: Image of trap aperture and electrodes after isotropic Si etch, showing the extent of the recessed Si. The sample illumination and the extent of the recess gives rise to the apparent distortion of the electrodes around the aperture; this is merely an imaging artefact.*

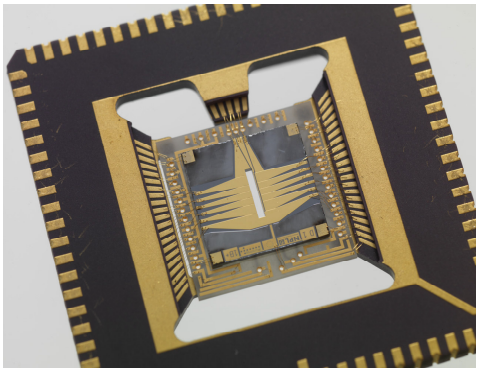

Fig. 11*: Monolithic silica-on-silicon trap chip mounted on CLCC chip carrier*

Gold-coated quartz 2D surface layer trap

A scalable approach that also uses lithography and which is more straightforward in fabrication terms, is a 2D (or surface) trap. Such traps have a relatively weak trapping potential but are easier to fabricate and provide a good architecture for demonstration of QIP operations such as shuttling, entanglement and gate operations. Oxford designed and fabricated such a trap based on gold-coated quartz [2]. Photolithography, metallisation and electroplating are required to create the 2D electrode structure. Figure 12 outlines the design of the Oxford surface trap and figure 13 shows the packaged trap.

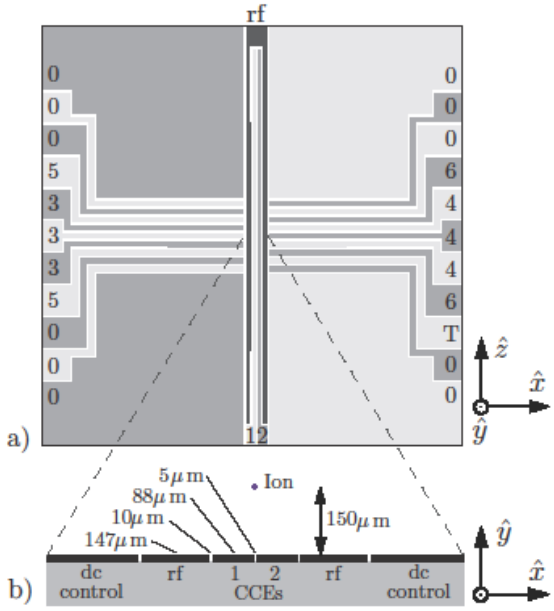

Fig 12: *Design layout of 2d surface trap*

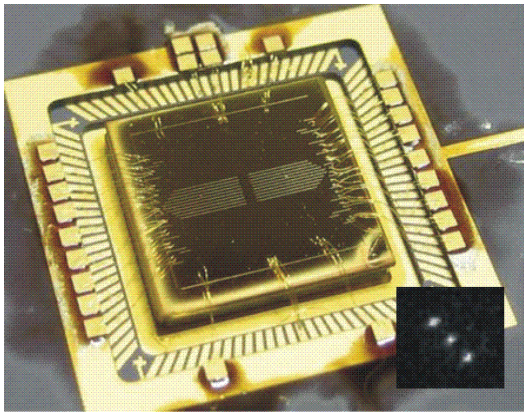

Fig. 13. *Packaged surface trap, wire-bonded onto chip-carrier, (inset) an image of a crystal of three cold ions trapped 150μm above the surface*

[2] A surface electrode ion trap with symmetric 4-wire geometry
D.T.C. Allcock et al., submitted for publication (see www.arxiv.org).

Microtrap drive and control interface

Control of noise-generating processes on electrodes is important for microtrap operation in order to avoid excessive heating rates, which scale inversely as the fourth power of ion-electrode distance. Such noise can arise in a wide variety of ways; this project has addressed the RF trap drive and control of DC electrodes. RF drive cleanliness is a basic requirement and and helical resonator drives generally provide the cleanest drive frequencies, but are not readily frequency tunable. Siegen have designed drive circuitry that allows this tunability, based on interchangeable crystal oscillators or a phase-locked-loop locked to a digital frequency generator. They have also developed in-vacuum gold-printed resistor and capacitor banks to provide the low pass filtering for low voltage feeds to the microtrap DC segmented electrodes. The developed 24 MHz drive circuitry gave excellent noise and harmonic suppression (53 dBV). For DC control, USIEG also demonstrated a single-channel fast FPGA-controlled DAC prototype with an impressive update rate of 20 MHz, which has the potential to be scaled to 100 channels.

In anticipation of scaling, the design evolved during the latter stages of the project, such that each DC electrode has its own DAC, each DAC its own memory and the DAC array can be controlled by multiple FPGAs to reduce the data transfer rates. This offers an extendable multi-FPGA / D-to-A design for multi-segment electrode control, essential for fast shuttling of ions between electrode segments. Siegen's "Electric Field Generator" design now incorporates a "motherboard – multi-daughter board" approach with up to ten daughter boards, each providing 2 channel outputs, resulting in a 20-channel device. This second prototype demonstrated improved linearity, generation of versatile potentials, and 4 channels have been tested on a single motherboard. This system has a 20 MHz update rate, is precise (to 1 mV up to 15 Vpp) and low in noise (<±0.5 mV). Ulm have also constructed a device for the control of DC electrodes. Using a Virtex 5 FPGA board, fast addressing of 64 control electrodes has been achieved. The update rate of 250 kHz and the number of channel were sufficient to demonstrate basic shuttling operations, but it is desirable to improve on the noise and speed specifications.

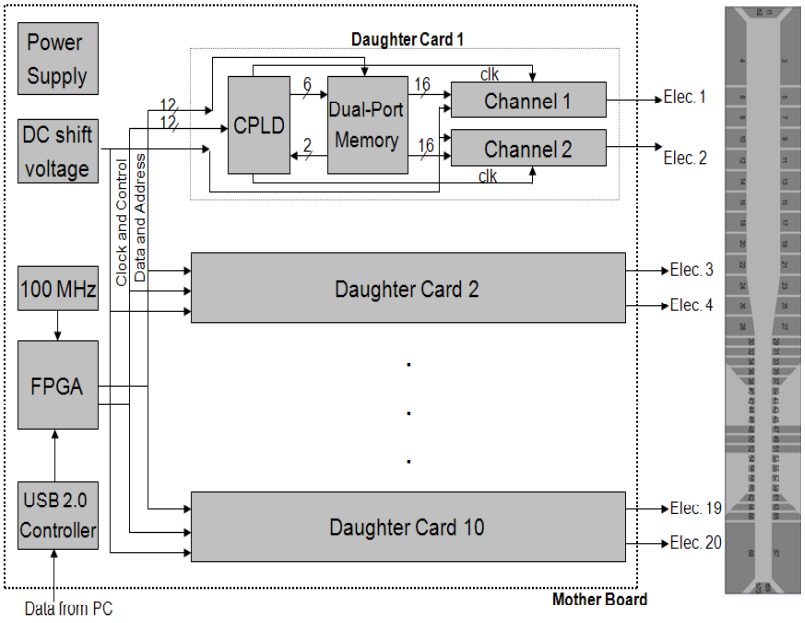

Fig. 14. *Architecture of Electric Field Generator device*

Microtrap connectivity across the vacuum interface

Recognising the need to integrate the ultra-high-vacuum environment needed for low decoherence microtrap chip operation together with the delivery of drive voltages and currents to the multiple electrical connections of the segmented trap, this requires an efficient arrangement for vacuum feedthrough of electrical connections to the trap chip. The voltages and currents necessary for the microtrap operation include rf voltage feeds (ideally well-separated from dc connections), compensation voltage feeds, shuttling control voltages, oven current and, in some cases, high current for magnetic field gradient generation to provide spatially dependent qubit transition frequencies, and microwave-radiation for driving the qubit. Paramount to achieving this is the high desirability of making use, where possible, of industry standard sub-components such as CCLC (ceramic leadless chip carrier) and CGPA (ceramic pin grid array) chip carriers.

As a result, we have developed a range of techniques for microtrap mounting on industry-standard chip carriers, allowing direct, interchangeable easy-access chip connectivity into the ultra-high-vacuum environment needed for the microtrap, which interfaces directly with standard micro-electronics design. Free-space optical access to the trap for laser cooling and fluorescence detection is provided by a window mounted with indium seals directly on to the chip carrier. This is an example of a "lab-on-a-chip" approach, but with the significant added capability of direct control and manipulation at the single particle quantum state level.

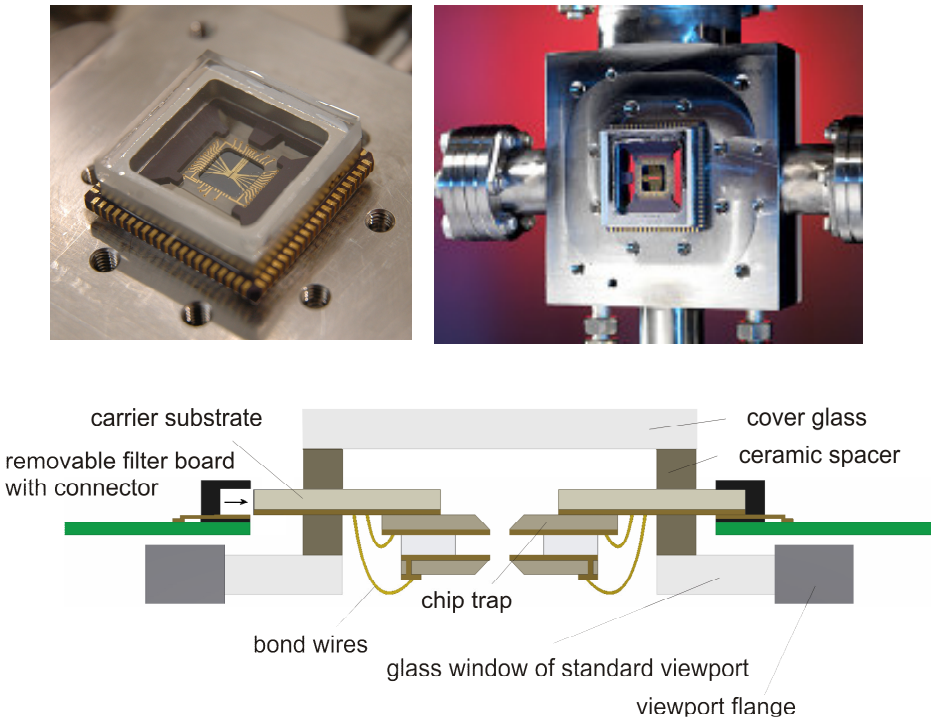

Fig 15: *UHV-compatilble microtrap chip carrier approaches using industry standard chip carriers, including NPL CLCC arrangement (top), and Innsbruck compact feedthrough (bottom).*

The Siegen feedthrough arrangement requires also to provide high current feeds for the magnetic field gradient and the use of non-magnetic elements to ensure good field stability. This precludes the use of standard chip carriers which use magnetic materials. In this case, the

custom chip carrier uses a thick film printing technique on aluminium oxide (Al_2O_3) with a thickness of 0.6 mm. Thick film printing allows easy design of complex circuitry containing resistors and capacitors for low pass filters positioned very close to the trap. The high current drives are achieved via copper heatpipes that also provide the mechanical support for the carrier. The layout is shown in figure 16.

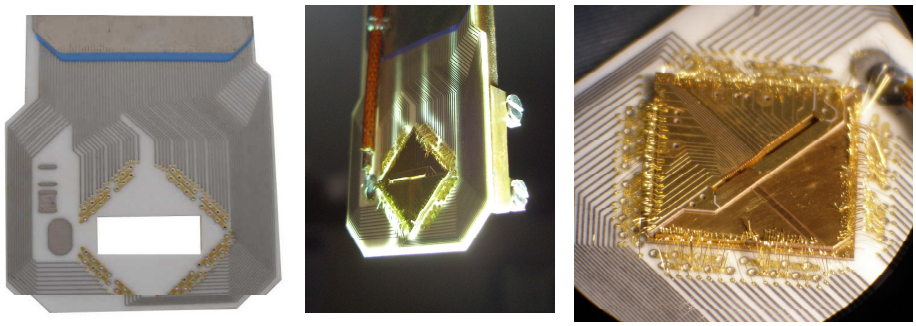

Fig. 16: *Thick film printed chip carrier for the Siegen magnetic field gradient trap*

In order to accommodate the Aarhus trap design concept, this also requires optical fibre feedthroughs into the vacuum system, in addition to standard electronic and optical access. This is achieved via a vacuum flange that accommodates a standard ceramic chip carrier, but also provides both electrical and fibre optic connectivity into vacuum. The feedthrough system is based on a titanium DN40CF UHV flange. Grooves milled into the chip carrier and flange allow optical fibres to enter the vacuum chamber, and the chip carrier itself acts as an electronic feedthrough. Free-space optical access is via a window mounted on a titanium spacer epoxied onto the opposite side of the chip carrier. Vacuum seals are created using a vacuum-compatible epoxy. Titanium is used as its thermal expansion coefficient is well matched to that of alumina.

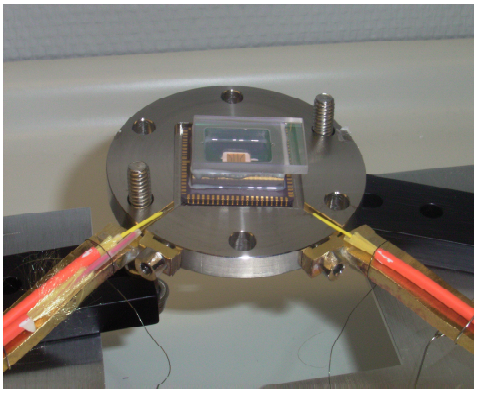

Fig. 17*: Au-on-Al_2O_3 microtrap mounted on UHV flange incorporating optical fibres*

Controlled ionisation and microtrap loading

Decoherence through noise generation can result from thermal electric fields, charge build-up on insulating surfaces and patch potentials due to contamination of electrode material by trapping species. One way to reduce this is loading by photo-ionisation. Novel methods for photo-ionisation and cooling laser beam delivery to the microtrap have been studied. Aarhus have demonstrated an ablation-based oven source for trap loading [3]. Also, lensed optical fibres have been developed for delivery of photo-ionisation and cooling light to the microtrap.

Aarhus developed a micro-scale oven for loading microtraps with calcium ions using a pulsed Nd:YAG laser to ablate calcium atoms from a pure metal target and then to photo-ionise these in situ using photo-ionising light at 272nm, delivered by UV-transmitting fibre (albeit with only a few percent transmission at this wavelength) with the custom lensed arrangement. The laser system has a maximum pulse energy of 80μJ and pulse durations in the region of 30-50ns. The 272nm laser light is derived by frequency quadrupling light from a distributed-feedback fibre laser [4]. In order to ablate material that predominantly comprises atoms in the ground state, it is necessary to use relatively low laser fluences, so that the ablation process is thermally driven. The calcium ion loading by laser ablation and photo-ionisation [5] was characterised by means of tests on a macroscopic ion trap.

The ablation-based oven source has been installed within the microtrap UHV vacuum chamber (figure 18). The pulse laser fluence is high enough to reach plasma formation threshold on the surface of the Ca-metal target inside the oven. The presence of ablated atoms was detected by driving the oven above the plasma formation threshold and observing a correlated increase of the background gas pressure inside the vacuum chamber, and the production of ions by using the trap electrodes as Faraday cups. Full operation of the microtrap with ablation oven-based loading is currently under investigation.

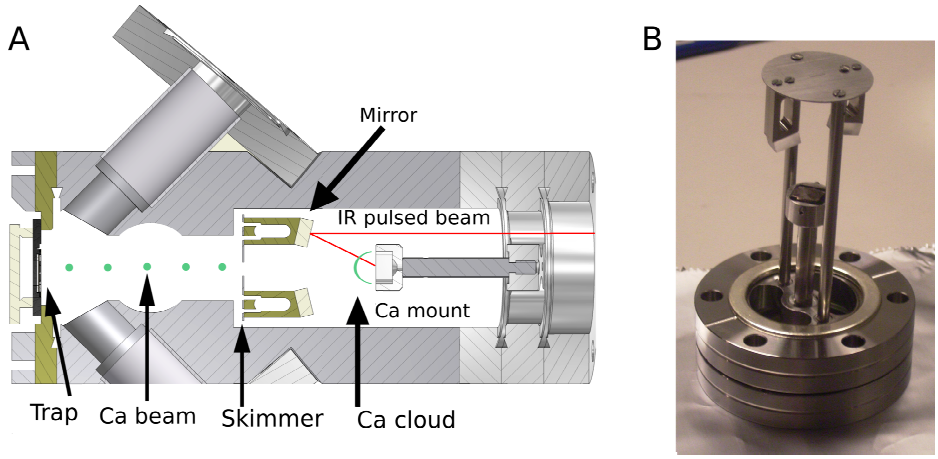

***Figure 18**: CAD drawing of the vacuum chamber illustrating the atom loading scheme. The path of the ablated atoms from the calcium target to the trap is illustrated (A). Picture of the fully assembled ablation oven just before installing it into the UHV system (B).*

[3] *An all-optical ion-loading technique for scalable microtrap architectures,* Applied Physics B **88**, 507 (2007)

[4] Second-harmonic generation of light at 544 and 272 nm from an ytterbium-doped distributed-feedback fiber laser Optics Letters **32**(3), 268 (2007)

[5] *Loading of large Coulomb crystals into a linear Paul trap incorporating an optical cavity for cavity QED studies*, Applied Physics B **93**, 373 (2008)

Single ion addressing and detection

Spatially-resolved optical addressing and detection of single ions within the linear string, together with fast quantum state read-out, are necessary for fast and unambiguous processing of gate operations. Single ion detection is generally achieved using sensitive high-resolution CCD cameras, and these have been instrumental in routine observation of ion strings within a number of ceramic wafer and surface microtrap arrangements early on in the project.

In respect of selective ion addressing, Siegen have demonstrated an optical-rf double resonance technique [6] [7] to individually select ions within a linear string of laser cooled $^{172}Yb^{+}$-ions trapped withinin a macroscopic linear Paul trap with magnetic field gradient. The ions were optically pumped into a dark metastable state $D_{3/2}$ ($m_J = \pm 3/2$) which has a lifetime of 52.2 ms. The Zeeman-manifold degeneracy is lifted by a total magnetic field B comprising an offset field plus field gradient. Magnetic dipole transitions are driven at a frequency

$$f = g_J \mu_B B / h \qquad (1)$$

with Landé g-factor g_J, and Bohr magneton μ_B, where the frequency is dependent on ion position in the field gradient. Selective observation of fluorescence from each ion is achieved for different rf frequencies, which transfer the ions into the bright $D_{3/2}$ ($m_J = \pm 1/2$) state.

The inhomogeneous field along the trap axis is created by cylindrical Nd-permanent-magnets. Figure 19 shows spatially resolved images of a string of four ions taken with an intensified CCD camera while setting the rf frequency to specific values that correspond to individual ionic resonances. The first and last image are taken without optical pumping and rf fields. The images in between (obtained with rf optical double resonance), show that single ions are selectively re-pumped by setting the rf frequency to a particular individual ionic resonance. Here, the spatial separation of the outer ions is 61.3 μm, corresponding to a gradient of 0.24 $T.m^{-1}$ for this particular demonstration.

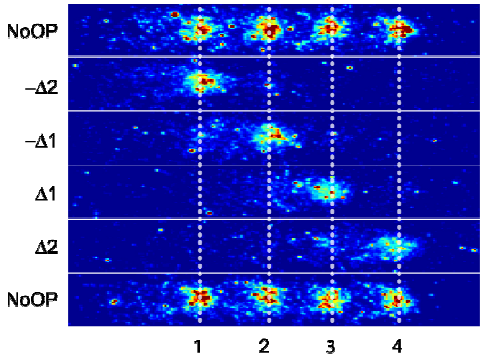

Fig 19: *RF optical double resonance imaging of a string of optically pumped ions exposed to an inhomogeneous magnetic field. The rf field was detuned from the single ion resonance frequency by Δ1 = 26.3 kHz and Δ2 = 83.2 kHz.*

Although the measurements presented here were performed in a macroscopic Paul trap, they allow estimation of parameters needed for use in the microtrap trap with miniaturized anti-Helmholtz-coil design. In this latter case, the gradient and therefore the frequency separation, should be boosted by a factor x200, allowing frequency separations of 20 MHz to be observed and reducing cross talk to a negligible level.

---

[6] M. Johanning, A. Braun, N. Timoney, V. Elman, W. Neuhauser, Chr. Wunderlich, Physical Review Letters **102**, 073004 (2009).

[7] M. Johanning et al., J. Phys. B: At. Mol. Opt. Phys. **42** (2009).
Individual addressing of trapped ions and coupling of motional and spin states using rf radiation

The standard technique for state determination is electron shelving, whereby ion population in the two qubit states is transferred to two different energy levels, only one of which is affected by rapid transitions. Observation of fluorescence on this transition therefore discriminates between the two qubit levels. The readout time is thus related to the ratio of the detected fluorescence rate to the noise introduced by scattered light and detector dark counts.

Critical to short gate times is the need for reduced state projection and qubit read-out times. Oxford used time-resolved fluorescence detection to make a critical test of single-ion readout fidelity. The time-resolved detection allows two important advances over the standard "photon-count threshold" qubit detection method (where *n* photons counted in a set time period are measured and the ion is inferred to be in a "bright" or "dark" state depending on whether *n* is above or below a fixed threshold). These are:

- discrimination of dark>bright or bright>dark events that fool the simple threshold method.
- adaptive detection, which terminates detection at a set statistical confidence level and results in significantly faster average qubit readout times.

With these time-resolved detection techniques, Oxford achieved 99.99% single-shot read-out fidelity in ~ 150 μs for an optical qubit in Ca^+ , more than ten times better than other methods [8], and important for fault-tolerant QIP and measurement-based quantum computing.

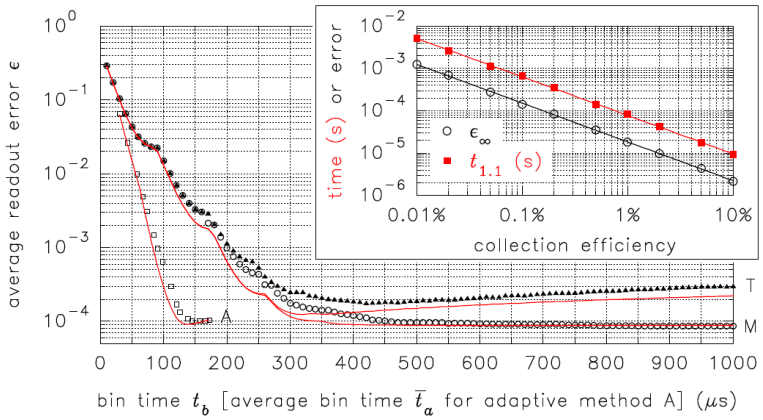

Fig 20: *Average readout error versus detection time for the $^{40}Ca^+$ optical qubit. Symbols are experimental data from 10^6 readout trials. Curves are simulations of 10^9 trials using ideal Poisson statistics. The inset shows how the readout error and time would both improve with higher photon collection efficiency.*

Oxford have now extended this work on high-fidelity single-qubit readout to a multi-qubit register[9], by accessing both spatial and temporal dimensions. With an electron-multiplying CCD, they demonstrated 99.99% single-shot readout fidelity for a multi-qubit register, in spite of optical cross-talk between neighbouring qubits at the level of ~4%. For a single qubit, they achieved 99.991(3)% single-shot fidelity in 400μs exposure time, limited by the qubit's decay lifetime. For a four-ion string, where the effect of decay was excluded by post-selection of data, they measured 99.999(1)% fidelity per qubit. A study of the cross-talk indicates that the method should scale to ~10000 qubits spaced ~1μm apart, with readout time ~1μs/qubit. Since the cross-talk is found only to affect nearest neighbours, this is scalable to 1D or 2D arrays of ions with negligible loss of fidelity.

---

[8] *High-fidelity readout of trapped-ion qubits* A.H. Myerson *et a.*, Phys. Rev. Lett. **100**, 200502 (2008).

[9] *Scalable simultaneous multi-qubit readout with 99.99% single-shot fidelity*
A.H. Burrell *et al.*, accepted for publication in Phys. Rev. A.

Ultra-fast ion transport and cross-trap shuttling

Critical to segmented microtrap operation is the ability to shuttle ions between segments in a controlled manner by means of time and amplitude variable dc potentials applied in sequence to the dc electrode segments. Practical shuttling algorithms that can achieve this without inducing heating and decoherence are essential for future QIP entanglement-based operations.

Based on the initial numerical work [10] [11], Ulm realized ultra-fast transport of single ions in a printed-circuit-board linear segmented trap. Within only very few oscillation periods they transported a single ion over 2 mm and back in 30µs. The ion motional excitation was monitored by a Doppler re-cooling measurement. The recovery of fluorescence only after a certain Doppler cooling time can be used to determine the ion's kinetic energy after the transport (Fig. 21) [12]. Repeating similar measurements with a microtrap with an axial frequency 5x higher and much narrower segments and thus a better overlap of the potential, and with an ion initially in the motional ground state, should enable further decreased transport time.

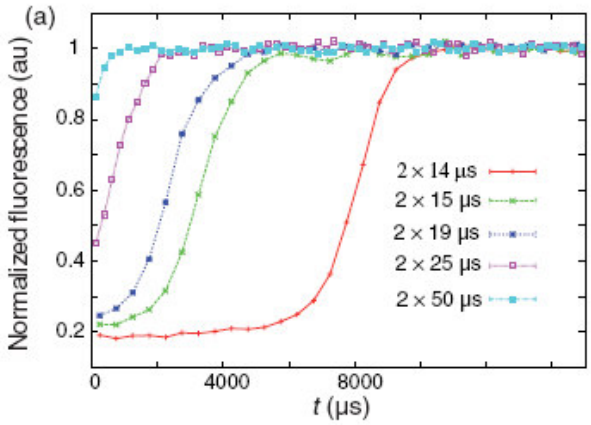

Fig 21: *Doppler re-cooling measurements for a single ion after an ultra-fast transport. The faster the transport, the higher the motional excitation and the longer the re-cooling time.*

Ulm have now realised ultra-fast transport of single ions in a linear gold-on-ceramic microtrap. The ions have been transported up to 0.8 mm in a time of 300 µs, using 75 steps where all 64trap electrode voltages are updated simultaneously. They have realized spectroscopy of ions "in the dark", where the ion is prepared in the loading segment, shuttled to a remote segment where a laser pulse at 729 nm excites the ion on one of the sidebands, measuring locally the trap frequency. The ion is then transported back in front of the fluorescence imaging optics to detect its internal quantum state, S or D. If the remote excitation was successful, the ion will be found in the non-fluorescing state. In this way, the spatial variation of trap frequencies can be mapped. For this remote spectroscopy to be useful, it is important that the transport ramps are fast enough, and indeed with the fast shuttle the data acquisition rate is not that different from read-out from a static ion.

[10] R. Reichle, et al.,"Transport dynamics of single ions in segmented microstructured Paul trap arrays", Progress of Physics, Wiley 54, No. 8 - 10, 666 (2006).
[11] S. Schulz,et al., "Optimization of segmented linear Paul traps and transport of stored particles", Progress of Physics, Wiley 54, No. 8 - 10, 648 (2006).
[12] G. Huber, et al., "Transport of ions in a segmented linear Paul trap in printed-circuit-board technology", New Journal of Physics 10, 013004 (2008).

Innsbruck developed a theoretical methodology to optimise electrode segment voltages for smooth transport of ions, and successfully applied it to shuttling round the junction of the cross trap design for the microtrap ceramic wafer chips. Simulations show that moving the trap potential at constant speed, the ion's motion is gradually converted into an oscillation along the y-axis as the trap potential is shifted around the corner. For an ion–trap electrode separation of 250 µm, the ions are shuttled along the quarter circle within 100 µs, and it can be shown that a longitudinal excitation amplitude of 150 µm (10-15 quanta) should be expected. This leads to the anticipation that optimised shuttling can produce negligible heating, critical for distribution of QI in segmented ion traps

Re-ordering of an ion string is critically dependent on the ability to transport ions. Recently, Innsbruck studied a two-ion crystal in a printed-circuit-board surface trap, and have manipulated the trapping potential beyond the standard linear geometry. They have established rotation of an ion string, and demonstrated deterministic reordering of a two-ion crystal, by means of a "three point turn". During this process, the ions leave the RF null for short times. This turns out to not seriously heat the ions, which is significant for shuttling around a cross trap corner. Innsbruck have also investigated theoretically the application of this technique to other trap designs, and found that it can be applied to standard 3D traps, such as the gold-on ceramic microtraps.

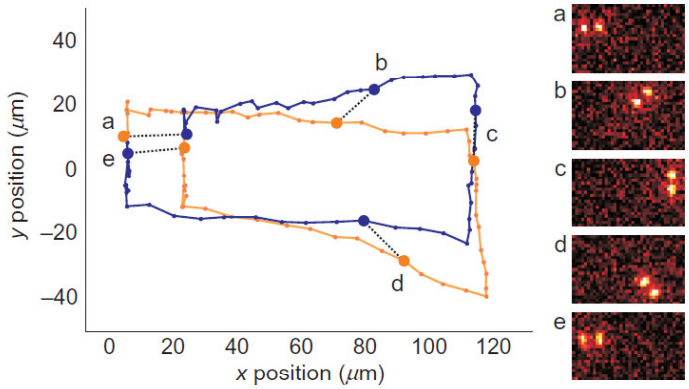

Fig 22: *Deterministic re-ordering of a two-ion crystal in a surface trap*

Innsbruck have also investigated theoretically the application of this technique to other trap designs, and found that it can be applied to standard 3D traps, such as the gold-on ceramic microtraps. The rotation of an ion string can thus be used universally in segmented ion trap quantum computing in order to sort and select ion qubits for quantum state transfer between ion registers. In addition, it has significance for sorting ions in a string when different isotopes or species of ions are used, e.g. for sympathetic cooling [13].

[13] F. Splatt, M. Harlander, M. Brownnutt, F. Zähringer, R. Blatt, and W. Hänsel, *Deterministic reordering of $^{40}Ca^{+}$ ions in a linear, segmented Paul trap,* New J. Phys. 11, 103008 (2009).

Cooling, heating & decoherence

The ability to cool and prepare ions in the motional ground state is one prerequisite for ion trap QIP. Equally important is the achievement of sufficiently low heating rates and decoherence, which determines how useful a specific microtrap technology will be.

Ulm have studied Raman transitions on a spin qubit in $^{40}Ca^{+}$ using a multi-segment gold-on-ceramic trap. Following resolved sideband cooling, they have measured the ion heating rate to be 0.3 phonons/ms; this is a factor of 10 improved over the value in the previous reporting period. In addition, they have demonstrated a new scheme for initialisation of the $^{40}Ca^{+}$ qubit via the $S_{1/2}$ –$D_{5/2}$ transition with a 99.6% fidelity; this is significantly better than what can be achieved by optical pumping on the cooling transition.

Oxford have measured the heating rate of $^{40}Ca^{+}$ in their surface trap, and found that the resulting electric field spectral noise density was comparable to that of other traps of the same size scale. A surface trap can only be addressed by cooling laser beams in 2D, to avoid unwanted scattered photons, therefore conventional techniques cannot compensate micromotion perpendicular to the trap plane. Oxford developed a novel method to do so, using coherent transitions driven by the repumper and cooling laser. The spectral noise density observed corresponds to a heating rate of ~ 50 quanta $m.s^{-1}$. In a separate experiment, they also investigated methods for protecting a single $^{43}Ca^{+}$ "memory qubit" against environmental decoherence. By using a sequence of "dynamic decoupling" pulses, the coherence time of the memory qubit increased by a factor of ~50, in the presence of dephasing noise arising from environmental magnetic field fluctuations.

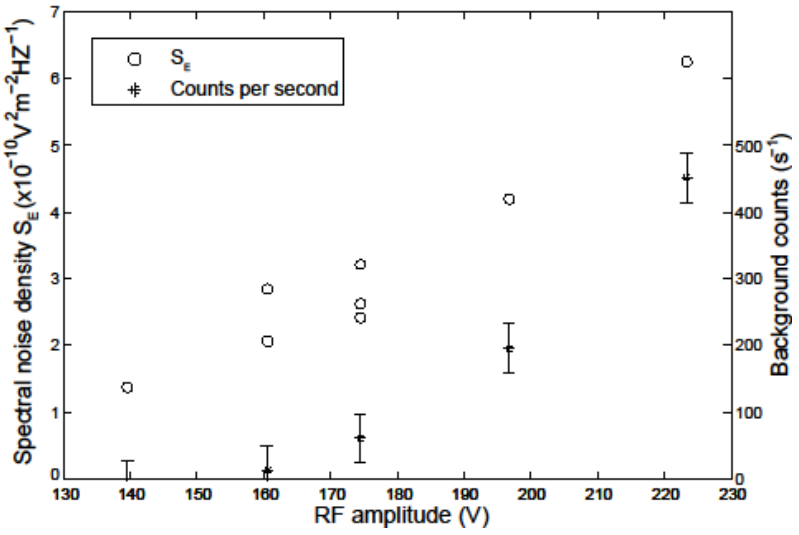

Figure 23*: Heating rate measurements of the Oxford surface layer trap, showing (open symbols) the electric field noise deduced from the motional heating of the ions as a function of RF trapping voltage amplitude. A faint background "glow" was also observed from the electrodes which may be associated with the heating.*

Ulm have studied Raman transitions on a spin qubit in $^{40}Ca^{+}$ using a multi-segment gold-on-ceramic trap. Following resolved sideband cooling, they have measured the ion heating rate to be 0.3 phonons/ms; this is a factor of 10 improved over the value reported previously. In addition, they have demonstrated a new scheme for initialisation of the $^{40}Ca^{+}$ qubit via the $S_{1/2}$ –$D_{5/2}$ transition with a 99.6% fidelity. This is significantly better than what can be achieved by optical pumping on the cooling transition.

Ulm have demonstrated improved sideband cooling close to the vibrational ground state and use Rabi oscillations on the blue motional sideband to extract the phonon number distribution. The dynamics of this distribution are analyzed to deduce a trap-induced heating rate of 0.3(1) phonons/ms. This is a factor of 10 better than previously reported [14]. This current value of 1 phonon every 3ms represents a time scale that is much slower than transport times of a few 100 µs and gate times. This improvement was due to lower noise driving electronics of the trap control electrodes. Further improvements should be possible here, allowing to reach a lower fundamental limit of surface patch field-induced ion heating. The measurement not only determines the mean phonon number but also checks that the phonon distribution is consistent with the thermal distribution.

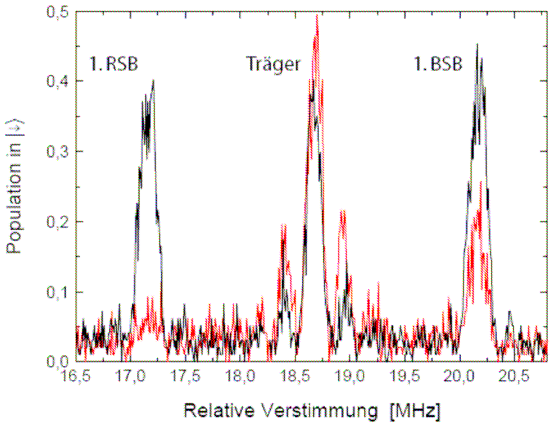

***Fig 24**: Spectroscopy of Raman Sideband with and without Raman ground state cooling of the axial mode of a single ion.*

Innsbruck have recently successfully operated one of the gold-coated ceramic layer cross traps and have observed Rabi flopping, but have not yet been able to make heating and decoherence rate measurements.

The proximity of dielectrics is a known limitation in its influence on a trap potential. This problem can be acute for a surface trap, given the ease with which the ion above the trap surface can be displaced as a result of charge build up on a nearby insulating surface. It is also relevant to traps in small chambers where the viewing windows are close to the trap. Innsbruck have investigated surface trap performance as a function of proximity to a glass plate, using the trapped ions' behaviour as a quantitative measure of the effect. Two different effects were seen to contribute. As the plate was moved close to 1 mm from the trap surface, oscillations in ion position set in, attributed to variable charge build-up on the plate due to UV irradiation. Further, charge build-up due to patch effects on the surface conducting layers plays an additional role. Establishing the boundaries of operation eg in terms of minimum acceptable distances to insulating surfaces, will play a significant role in determining the optimal trap design and environment.

[14] *Sideband cooling and coherent dynamics in a microchip multi-segmented ion trap*
S. Schulz, U. Poschinger, F. Ziesel and F. Schmidt-Kaler, ", New Journal of Physics **10**, 045007 (2008)

Entanglement and Gate operations in microtraps

The routine deployment of entanglement and gate operations are pre-requisites for QIP. Whilst substantial results have been achieved in recent years for macroscopic traps in both these areas, the carry-over to microtrap architectures represents a more difficult step, on account of both fabrication issues and higher expected heating rates associated with reduced ion-electrode separations. However, some preliminary but impressive ion and state manipulation techniques have been achieved.

Entanglement studies targeted, in the first instance, the controlled positioning of ions in proximity to each other using shuttling techniques, followed by separation operations, as preliminary to demonstration of basic 2-ion entanglement, leading to subsequent entanglement transfer to other ions and state teleportation. Further it was intended to measure the fidelity of the entanglement process at each stage, together with decoherence times.

Ulm achieved the deterministic loading, positioning and splitting of ions within a string, as a precursor to entanglement demonstration. Whilst they have typically relied on pre-determined voltage ramps for ion transport, recently they investigated novel schemes where the accurate observation of ion positions is used to close a feed-back loop, thus actively controlling the trap parameters. This is important since it has been reported that minor day-to-day variations in trap operating parameters require frequent re-calibration and modification of such pre-defined voltage ramps. In an active feed-back scheme no such operation is necessary. The feed-back positioning scheme realized offers a number of advantages. One of these is the splitting of linear crystals. The trap depth is reduced and one ion at the right hand side of the crystal is pulled out of the crystal while all other ions are kept in place.

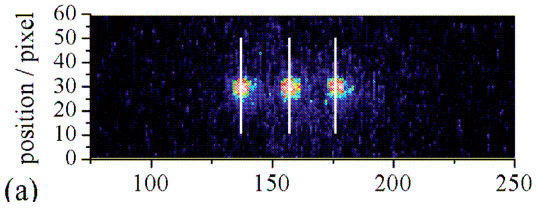

Fig 25: *CCD image-based positioning of ion crystals.*

A fast algorithm is used to determine the ion positions in a linear crystal from CCD images. The ion positions are subtracted from the desired positions to generate an error signal. Thus, the read-out of fluorescence images is used to control the ion position and configuration of the ion crystal with sub-µm precision within ms time scale. As a consequence of the active feed-back, the method is robust against fluctuations. This thus allows the separation of ion(s) from a string, followed by recombination with deterministic precision. An example is given in figure 26. this demonstrates an underlying robust ion transport sequence needed to deterministically entangle multiple ions within separate strings.

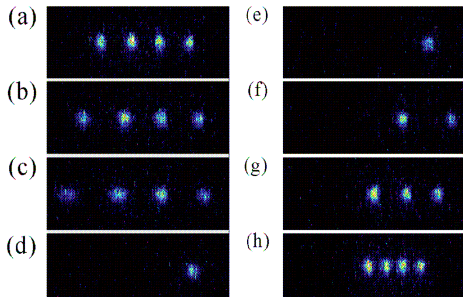

Fig 26: *CCD images of one ion split off from a four - ion crystal*

As a pre-cursor to gate operation Ulm have demonstrated basic operations required for gates within the ceramic wafer microtrap, using a spin qubit in $^{40}Ca^{+}$ [15]. The resolved sideband cooling and high-fidelity qubit initialisation mentioned earlier are the starting point. Ulm then use the Raman transition close to the $S_{1/2}$ - $P_{1/2}$ resonance at 397nm for coherent manipulation of the qubit and observed single qubit rotations with 96% fidelity and gate times below 5µs. Fig. 27 shows carrier Rabi flops on the Raman transition, with a Rabi frequency of ~ 1 MHz.

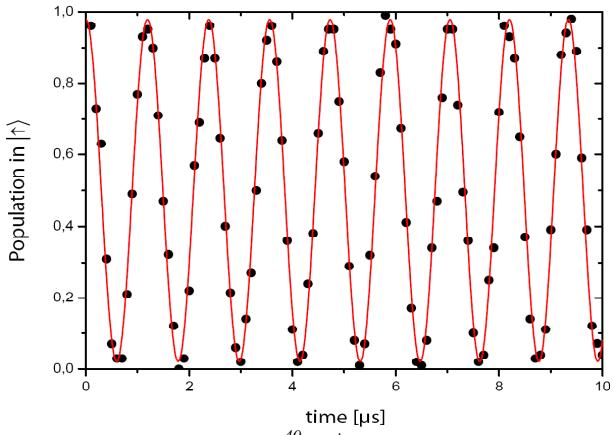

Fig 27: *Rabi oscillations on $^{40}Ca^{+}$ spin qubit Raman transition:*

They have also observed coherent (Rabi) oscillations on the Raman blue axial sideband after resolved sideband cooling on the optical $S_{1/2}$ to $D_{5/2}$ qubit transition. In addition, Ramsey spectroscopy has been performed on the Raman co-carrier transition, which is useful for monitoring internal state decoherence.

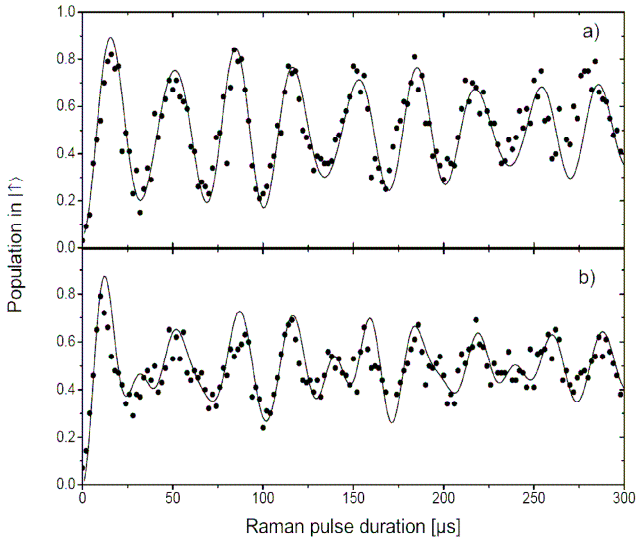

Fig 28: *Raman Rabi oscillations on the blue axial sideband (a) directly after resolved sideband cooling on the $S_{1/2}$ to $D_{5/2}$ transition and (b) after a waiting time of 3ms.*

[15] *Coherent Manipulation of a $^{40}Ca^{+}$ Spin Qubit in a Micro Ion Trap*
U. G. Poschinger, G. Huber, F. Ziesel, M. Deiss, M. Hettrich, S. A. Schulz, G. Poulsen, M. Drewsen, R. J. Hendricks, K. Singer and F. Schmidt-Kaler, J. Phys. B: At. Mol. Opt. Phys. **42**, 154013 (2009).

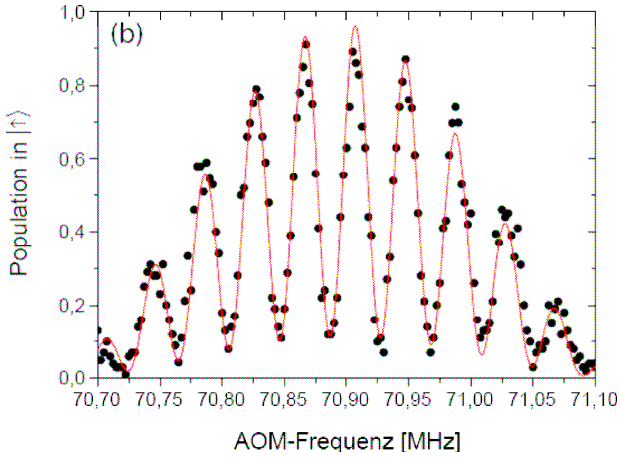

Fig. 29: *Ramsey spectroscopy fringes on the Ca+ Raman co-carrier transition*

With these techniques, the spin qubit coherence time has been determined to be around 2 ms, mostly limited by ambient magnetic field fluctuations.

Partner collaboration

Collaborations within and beyond the Microtrap consortium has included 2-day workshops, invited seminars and presentations at relevant international conferences. Microtrap workshops were held every 6 months at NPL (2006), Ulm and Innsbruck (2007), Siegen and Aarhus (2008) and Oxford (2009), together with a trapped ion workshop satellite meeting to ICAP in Innsbruck (July 2006). These enabled critical review of partner activities and crystallised forward thinking. A brief description of the Microtrap project together with highlights of the results can be found on the Microtrap website (www.microtrap.eu).

Conclusion

In conclusion, this project has developed a spectrum of technical capabilities that has only been possible through collaboration. The consortium has developed mirofabricated traps of three different design technologies; each is capable of addressing particular aspects of the challenges faced in scalability of trapped ion QIP. Hardware has been developed to interface the trap chips, eg for UHV, electrical and optical connectivity, and scalable high-speed electrical control. Some microtraps have been evaluated, and are now being used to demonstrate ion manipulations relevant to entanglement and quantum gates: *eg* coherent control of the qubit state, and accurate and precise control of ion transport trajectories. These are significant advances in addressing the challenge of ion trap scalability.

Microtrap Partners

NPL National Physical Laboratory, UK
UIBK University of Innsbruck, Austria
UUAR University of Aarhus, Denmark
UOXF University of Oxford, UK
USIEG University of Siegen, Germany
UULM University of Ulm, Germany